J Mater Sci: Mater Electron (2017) 28:2833–2837
DOI 10.1007/s10854-016-5866-6

Zn/ZnSe thin films deposition by RF magnetron sputtering

H. Hakan Yudar[1] · Suat Pat[1] · Şadan Korkmaz[1] · Soner Özen[1] · Volkan Şenay[2]

Received: 21 July 2016 / Accepted: 8 October 2016 / Published online: 14 October 2016

Abstract In this paper, Zn/ZnSe thin films were deposited on glass substrates by RF magnetron sputtering system. XRD analyses were done. Zn and ZnSe phases were obtained. Miller indices of obtained Zn phases were detected in (320), (620) and (112) crystal formation. For the ZnSe phases, only one peak of (110)/(220) was observed. The surface morphology of the samples was investigated by an atomic force microscopy tools. It found that average roughness of the films was increased by raised RF power. The thin films around 80 % of high transmittance were measured. The band gap values were calculated as to be ~2.80 eV by the Cauchy model. The calculated refractive indices values were approximately 2.25 by a relation between the refractive index and the band gap.

1 Introduction

II–VI semiconductor systems have many electronic and optoelectronic applications among inorganic semiconductor materials. Therefore, many researchers are strive to control the shape and size of the inorganic semiconductor. Researchers are working to understand their new features together with the structure relationship. zinc selenide (ZnSe) has well known II–VI semiconductor having direct band gap almost 2.7 eV. Therefore, the ZnSe films have low optical absorption, the high refractive index in the visible and infrared spectral region. These features show unique optical properties for some the potential applications, such as light-emitting diodes [1], photoluminescence [2] and electro-luminescent devices [3], lasers [4], thin film solar cell [5], nonlinear optical crystal [6] and infrared optical material [7].

ZnSe thin films are deposited by several techniques, such as RF magnetron sputtering (RF) [8], chemical vapor deposition [9], sol–gel process [10], thermionic vacuum arc (TVA) [11], molecular beam epitaxy [12], pulsed laser deposition [13], vacuum evaporation [14], electrodeposition [15] and etc.

In this work, the ZnSe thin films were generated by the RF magnetron sputtering. RF was used because this technique allows full control of the accumulation parameters and the desired quality material to be produced. The samples were deposited onto glass substrates at different powers. The effect of RF power on the structural, morphological and optical properties of deposited thin films on the substrates was investigated. The optical properties of the samples were examined by UV–Vis spectrophotometer. The samples were characterized by scanning electron microscopy (SEM), energy dispersive X-ray spectroscopy (EDX) and atomic force microscopy (AFM). With these techniques, respectively, the surface topography, the elemental analysis and the surface morphology of the film produced was conducted. XRD analysis was used for the evaluation of the microstructural properties.

2 Experimental

The materials used in this study, 99.9 % purity, with 2 mm thickness, in 50 mm diameter was bulk Zinc Selenide (ZnSe). The disk inserted in target section of sputter gun. The glass substrates were cleaned by ethyl alcohol and the

✉ H. Hakan Yudar
hakany@ogu.edu.tr

[1] Physics Department, Eskişehir Osmangazi University, Eskisehir, Turkey

[2] Education Faculty, Bayburt University, Bayburt, Turkey

surfaces were cleaned sequentially de-ionized water for 7 min and then cleaned glasses were allowed to air dry. After that, cleaned glasses were placed in the substrate holder. The distance between the substrates and the target was 30 mm and it was kept constant in deposition procedure. The chamber was vacuumed to the 10^{-2} Torr before the RF deposition process being started. Argon gas (99.99 %) were utilized for deposition of ZnSe samples. The ZnSe thin films were prepared by using RF magnetron sputter technique in the chamber. RF powers were applied as 50 W for sample 1 (S1) and 100 W for sample 2 (S2). The pressure of vacuum chamber was set to 3×10^{-1} Torr. The coating processes were conducted for 30 min under these conditions. All substrates were not heated while the film deposition. The films were produced at room temperature by argon plasma without post annealing process. The parameters used in this experiment are shown in Table 1.

3 Results and discussion

PANalytical Empyrean XRD tool was used for crystallographic characterization of the deposited ZnSe films at 50 and 100 W. Figure 1 represents the X-ray diffraction patterns of the produced films. As shown in Fig. 1, peaks in the XRD patterns were found for Zn and ZnSe for 50 and 100 W. Miller indices of Zn and ZnSe are (320), (620), (112) and (110)/(220), respectively. Debye–Scherrer formula is used to calculating of the grain sizes:

$$D = K\lambda/\beta\cos\theta \quad (1)$$

where D is the crystallite size, K, 0.94, is a shape constant, λ is used X-ray wavelength, β is the full width at half maximum (FWHM) of the observed peak and θ is the Bragg's angle of the selected peak [16, 17]. Average crystallite sizes for the films were calculated as 26 and 30 nm for the ZnSe peak of samples.

Also, microstrain values were calculated from the following Eq. 2:

$$\varepsilon = (\beta\cos\theta)/4 \quad (2)$$

where ε is the microstrain and β is full width at half maximum (FWHM) of the observed peak from Eq. 2 [18]. The number of crystallites per unit area (N) is given the following equation [19, 20];

Table 1 Production parameters of deposition process

Parameters	S1	S2	Unit
Pressure	3×10^{-1}	3×10^{-1}	Torr
Power	50	100	W
Time	30	30	min
Gas	Argon	Argon	–

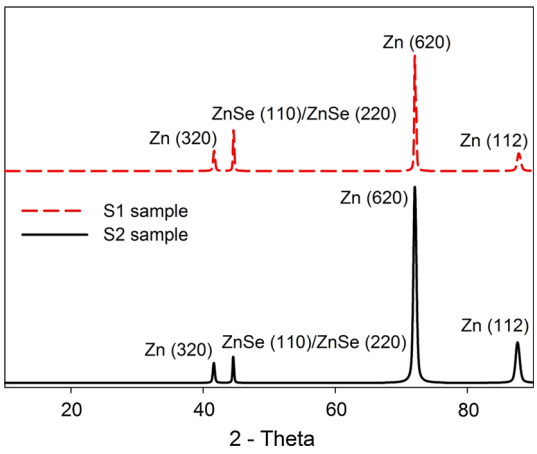

Fig. 1 XRD images for as prepared ZnSe films deposited at different power

$$N = t/D^3 \quad (3)$$

where t is the thickness of the films. The calculated results are shown in Table 2. Obtained results show that the number of crystallite size per unit volume is increased by the increasing RF power.

The surface roughness of the coated ZnSe has investigated over 2×2 m^2 scanning areas by AFM (Ambios Q-Scope) analysis. The AFM was used to get information about the surface topography of the ZnSe thin films. In Fig. 2 is shown the taken AFM images of the film coated surfaces at 50 and 100 W. Figure 2 shows the 1.5 and 22 nm average surface roughness results for the S1 and S2 samples. In Fig. 2a, b, 2D and 3D of S1 sample is shown images of coated ZnSe, respectively. In Fig. 2c, d, 2D and 3D of S2 samples are shown images of coated ZnSe, respectively. In the Fig. 2b, the AFM image showed that the coated ZnSe film surface has non-flat hilly features with sharp domes at the top. In the Fig. 2d, the AFM image of surface morphology has a non-flat summit and symmetric height-distribution.

Root mean square (RMS) refers to the roughness of the coated films. The increase of the RMS values means the rise of roughness. The mean RMS roughness was taken at different areas of each film at room temperature and atmospheric pressure. The RMS roughness of the sample films increased from 1.5 to 22 nm with the increase in coating power. Skewness (Ssk) and Kurtosis (Skr) are the important parameters to understand and measure the flatness and asymmetry of the films. If the Ssk value is equal to zero, A perfect symmetrical on the surface are observed. If the Ssk value is positive, the surface has more peaks than valleys and the height distribution is asymmetrical. If the Ssk value is negative, the surface is more planar and valleys are more predominantly. The surface has a normal distribution when values of the Skr shows zero. Surface

Table 2 Some parameters of XRD samples produced at 50 and 100 W

Samples	Thickness (nm)	Crystallite size (nm)	Lattice strain	Microstrain	Number of crystallites per unit volume (m^{-2})
S1	5	26	0.0039	0.063578855	2.84479E+14
S2	60	30	0.0034	0.061462606	2.26727E+15

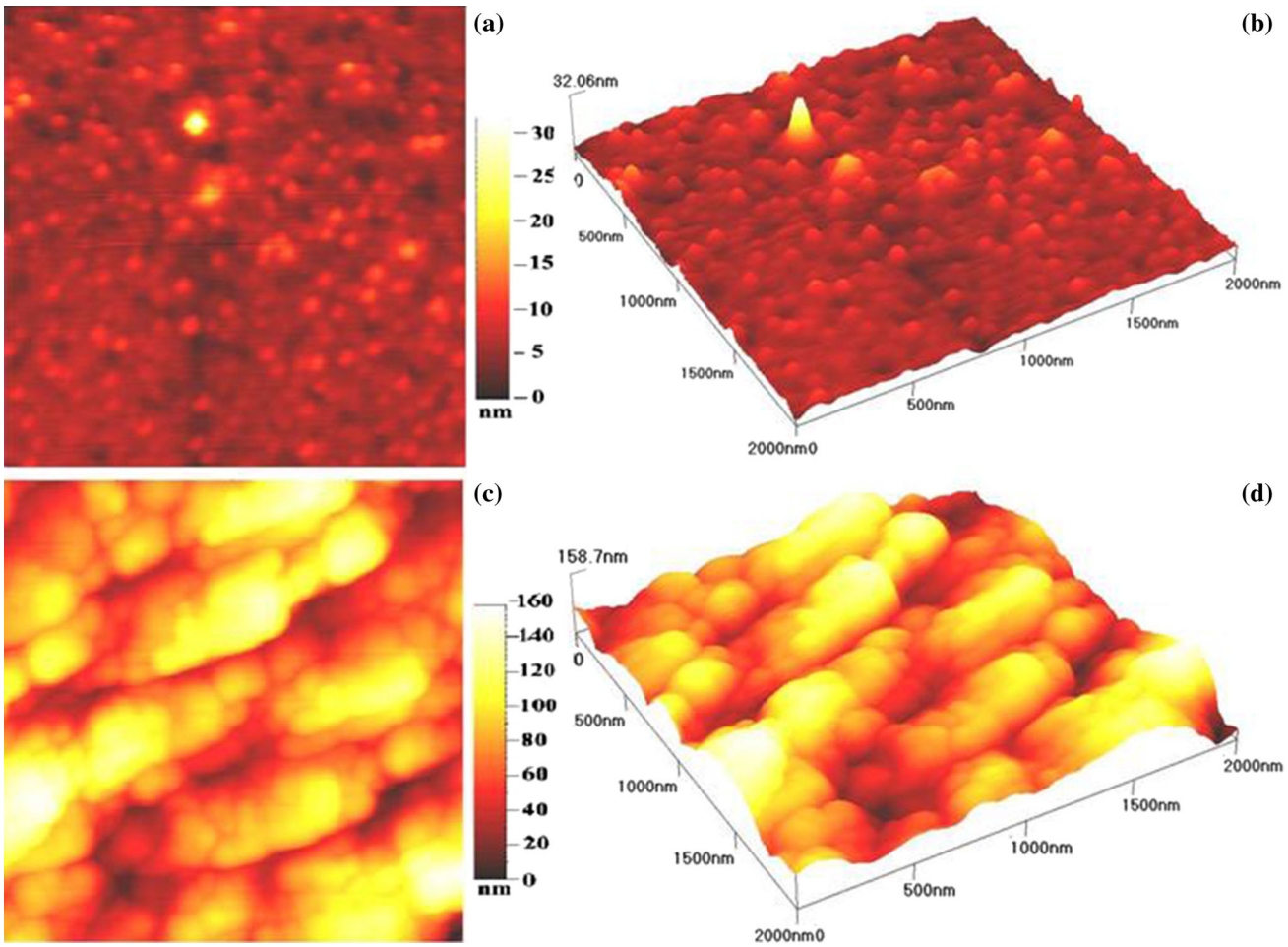

Fig. 2 Atomic force microscopic (AFM) images of deposition ZnSe **a** 2D, **b** 3D at 50 W and **c** 2D, **d** 3D at 100 W

morphology has a sharply peaked structure when the Skr shows positive value. Surface morphology has a flat-topped structure when the Skr shows a negative value.

Sample 2 has more surface roughness than sample 1. For both examples, the surface has more peaks than flatness and the height of peaks is asymmetrical. The surface structure of sample 1 has sharp peaked, but the surface structure of sample 2 has flat topped. The Ssk, Skr and RMS values of samples are shown in Table 3 with measured using AFM.

Some optical properties of the coated films are shown in Fig. 3. Transmittance and absorbance measurements of coated samples were performed with UV–Vis transmission spectroscopy (UNICO 4802 double beam). UV–Vis transmission spectroscopy was performed in the wavelength range of 200–1000 nm. Figure 3a shows a transmittance spectrum of coated ZnSe thin films. The optical transmittance values were recorded over 83 and 80 % in the near infrared region for sample 1 and sample 2, respectively.

Table 3 Surface characterization results of deposited samples at 50 and 100 W

Sample	RMS	Skewness (Ssk)	Kurtonis (Skr)
S1 (50 W)	1.888	2.123	14.645
S2 (100 W)	28.01	0.204	−0.305

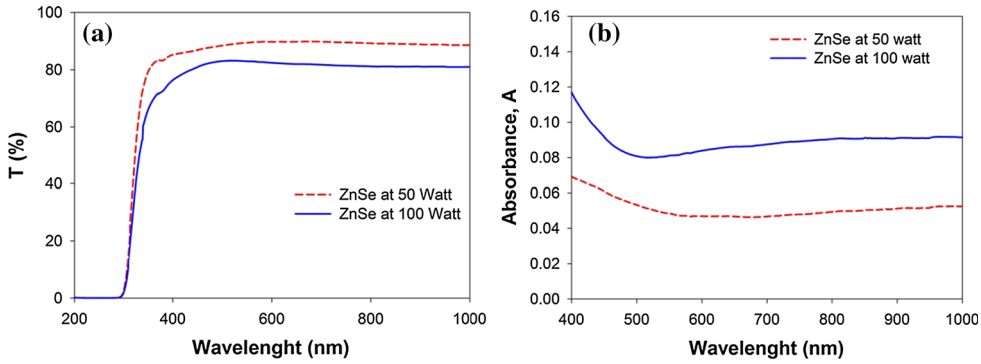

Fig. 3 **a** Transmittance and **b** absorbance spectrum of the samples ZnSe coated with at different power values

Figure 3b shows absorbance values spectrum of coated ZnSe thin films. The absorbance values were determined in the spectrometer. ZnSe thin films have direct band gap energy.

Direct band gap energy of ZnSe thin film is shown in the Fig. 4. The relationship between the absorption coefficients and photon energy is as follows:

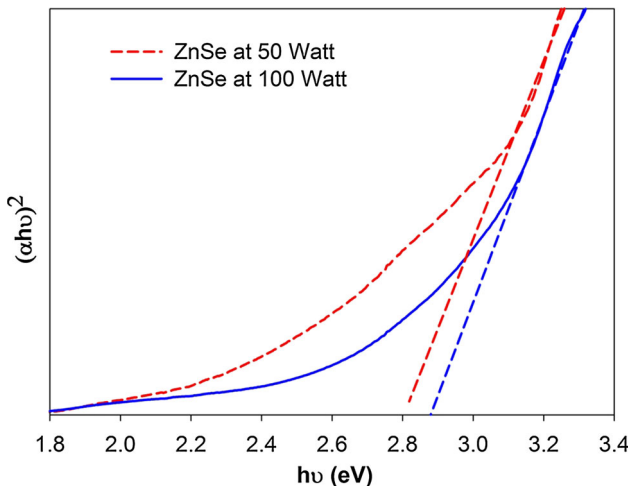

Fig. 4 $(\alpha h\nu)^2$–hν plots of the ZnSe coated samples at different power values

$$\alpha h\nu = A(h\nu - E_g)^n \quad (4)$$

where α is the optical absorption coefficient, hν (eV) is the incident photon energy, A is constant, n = ½ for direct transition, E_g (eV) is the optical band gap of the material [21, 22]. Figure 4 shows the plot of $(\alpha h\nu)^2$ against (hν) for ZnSe thin film from the optical spectra at different power values. According to Fig. 4, the band gap values of the coated films are nearly equal to about 2.8 eV for each sample. Obtained results are in good agreement with literature [23].

The refractive index (n) and the reflectance spectrum of samples (ZnSe) produced were measured using Filmetrics F20 interferometer and shown in Fig. 5. Only one surface of the glass substrates was coated and only coated surfaces were measured. The refractive index of ZnSe films produced at 50 and 100 W are plotted as a function of wavelength in Fig. 5a. The known values of refractive index are in good agreement with films deposited by magnetron sputtering (n ∼ 2.6 at 550 nm) [24]. Refractive index values of the coated films were over 2.56, 2.23 for 50 and 100 W at 550 nm, respectively.

As shown in Fig. 5b, the reflectance of the coated films were plotted at different power. It was determined that the average reflectance values of ZnSe coated onto glass substrates about 5.28 and 5.72 % for 50 and 100 W at 550 nm, respectively.

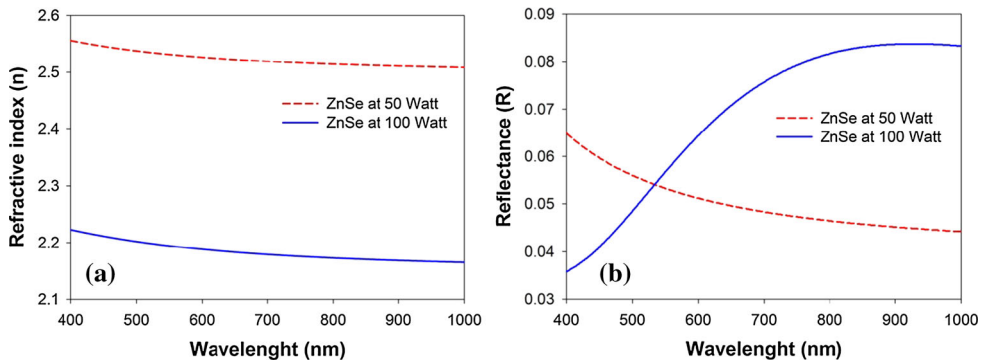

Fig. 5 Refractive index **a** of ZnSe films and **b** reflectance spectrum of ZnSe films at 50 and 100 W

There is a relation between the refractive index and the band gap. This equation is as follows:

$$n = \sqrt{\frac{12.417}{E_g - 0.365}} \quad (5)$$

where n is the refractive index and E_g is the band gap [25]. The calculated refractive index values are approximately 2.25.

4 Conclusions

In this paper, Zn/ZnSe thin films were produced at two different power by RF magnetron sputtering system. Zn/ZnSe crystallites structures were detected in XRD patterns. Crystallite size, lattice strain and microstrain values were reduced once increasing RF power. The number of the crystallite per unit volume values were increased by RF power. But, crystallite size values were nearly closed to each other. It concluded that the number of the crystallite per unit volume values changed the transmittance, refractive index and reflectance values of the deposited samples. The band gaps are in good harmony with the related literature.

References

1. J. Nishizawa et al., Blue light emission from ZnSe p–n junctions. J. Appl. Phys. **57**(6), 2210–2216 (1985)
2. Y.-H. Wu, K. Arai, T. Yao, Temperature dependence of the photoluminescence of ZnSe/ZnS quantum-dot structures. Phys. Rev. B **53**(16), R10485 (1996)
3. V. Wood et al., Alternating current driven electroluminescence from ZnSe/ZnS: Mn/ZnS nanocrystals. Nano Lett. **9**(6), 2367–2371 (2009)
4. D. Albert et al., Influence of p-type doping on the degradation of ZnSe laser diodes. Appl. Phys. Lett. **74**(14), 1957–1959 (1999)
5. Y. Ohtake et al., Polycrystalline Cu (InGa) Se2 thin-film solar cells with ZnSe buffer layers. Jpn. J. Appl. Phys. **34**(11R), 5949 (1995)
6. X. Du, et al., Generation of a dark hollow beam by a nonlinear ZnSe crystal and its propagation properties in free space: theoretical analysis. Opt. Commun. **322**, 179–182 (2014)
7. M.A. Pickering, R.L. Taylor, D.T. Moore, Gradient infrared optical material prepared by a chemical vapor deposition process. Appl. Opt. **25**(19), 3364–3372 (1986)
8. A. Rizzo et al., The influence of the momentum transfer on the structural and optical properties of ZnSe thin films prepared by RF magnetron sputtering. Thin Solid Films **368**(1), 8–14 (2000)
9. A. Reina et al., Large area, few-layer graphene films on arbitrary substrates by chemical vapor deposition. Nano Lett. **9**(1), 30–35 (2008)
10. E.I. Ko, Sol–gel process. Prep. Solid Catal. (1999). doi:10.1002/9783527619528.ch3e
11. M. Özkan et al., ZnSe nanocrystalline thin films deposition on Si substrate by thermionic vacuum arc. Proc. Inst. Mech. Eng. L J. Mater. Des. Appl. **226**(2), 103–108 (2012)
12. B.R. Pamplin (ed.), *Molecular Beam Epitaxy* (Elsevier, Amsterdam, 2013)
13. R. Eason, *Pulsed Laser Deposition of Thin Film: Applications-led Growth of Functional Materials* (Wiley, Hoboken, 2007)
14. T. Tsutsumi, Dielectric properties of Y_2O_3 thin films prepared by vacuum evaporation. Jpn. J. Appl. Phys. **9**(7), 735 (1970)
15. C. Ross, Electrodeposited multilayer thin films. Annu. Rev. Mater. Sci. **24**(1), 159–188 (1994)
16. V. Şenay et al., Some physical properties of a Si-doped nanocrystalline GaAs thin film grown by thermionic vacuum arc. Vacuum **119**, 228–232 (2015)
17. S. Özen et al., AlGaAs film growth using thermionic vacuum arc (TVA) and determination of its physical properties. Eur. Phys. J. Plus **130**(6), 1–6 (2015)
18. M. Ashraf et al., Effect of annealing on structural and optoelectronic properties of nanostructured ZnSe thin films. J. Alloys Compd. **509**(5), 2414–2419 (2011)
19. A. Purohit et al., Impact of low temperature annealing on structural, optical, electrical and morphological properties of ZnO thin films grown by RF sputtering for photovoltaic applications. Opt. Mater. **49**, 51–58 (2015)
20. H.H. Yudar, Ş. Korkmaz, S. Özen, V. Şenay, S. Pat, Surface and optical properties of indium tin oxide layer deposition by RF magnetron sputtering in argon atmosphere. Appl. Phys. A **122**(748), 1–6 (2016)
21. S. Özen et al., Some physical properties of the SiGe thin film coatings by thermionic vacuum arc (TVA). J. Nanoelectron. Optoelectron. **10**(1), 56–60 (2015)
22. S. Özen et al., Deposition of a Mo doped GaN thin film on glass substrate by thermionic vacuum arc (TVA). J. Mater. Sci. Mater. Electron. **26**(7), 5060–5064 (2015)
23. G. Agawane et al., Preparation and characterization of chemical bath deposited nanocrystalline ZnSe thin films using Na 3-citrate and hydrazine hydrate: a comparative study. Mater. Lett. **106**, 186–189 (2013)
24. G. Olbright et al., Microsecond room-temperature optical bistability and crosstalk studies in ZnS and ZnSe interference filters with visible light and milliwatt powers. Appl. Phys. Lett. **45**(10), 1031–1033 (1984)
25. R. Reddy et al., Optical electronegativity and refractive index of materials. Opt. Mater. **10**(2), 95–100 (1998)